

Electronic Supplemental Information

The Hydrogen Atom Transfer Reactivity of a Porphyrinoid Cobalt Superoxide Complex

*Jireh Joy D. Sacramento and David P. Goldberg**

Department of Chemistry, The Johns Hopkins University, 3400 N. Charles Street, Baltimore,
MD 21218, USA

*Email: dpg@jhu.edu

Materials. All chemicals were purchased from commercial sources and used without further purification unless otherwise stated. Reactions involving inert atmospheres were performed under an Ar atmosphere using standard Schlenk techniques or in an N₂-filled dry box. Dichloromethane and THF were purified via a Pure-Solv solvent purification system from Innovative Technologies, Inc. Anhydrous pyridine (py) was purchased from Sigma Aldrich. Deuterated solvents for NMR were purchased from Cambridge Isotopes, Inc. Dichloromethane, pyridine and deuterated solvents were distilled from CaH₂ then degassed by repeated cycles of freeze-pump-thaw and stored over 4 Å molecular sieves in an N₂-filled drybox prior to use. The synthesis of Co^{III}(py)₂(TBP₈Cz) (TBP₈Cz = octakis(*p*-*tert*-butylphenyl)corrolazinato)^{1,2} and 2,2,6,6-tetramethylpiperidine hydroxylamine (TEMPOH)³ followed published literature procedures. Diphenylhydrazine (DPH) was recrystallized twice in ethanol and dried under vacuum prior to use.

Instrumentation. UV-vis spectra were collected with a Varian Cary 50 Bio Spectrophotometer coupled to a Unisoku USP-203 Cryostat or a Hewlett-Packard Agilent 8453 diode-array spectrophotometer with an air-free quartz cuvette (3.5 mL, path length = 1 cm) fitted with a septum. ¹H NMR spectra were recorded on a Bruker Advance 400 or 300 MHz FT-NMR spectrometer. Electron paramagnetic resonance (EPR) spectra were recorded with a Bruker EMX spectrometer equipped with a Bruker ER 041 X G microwave bridge and a continuous-flow liquid helium cryostat (ESR900) coupled to an Oxford Instruments TC503 temperature controller for low temperature data collection.

Generation of [Co^{III}(py)(O₂)(TBP₈Cz)]⁻

a) UV-vis spectroscopy. To a solution of Co^{III}(py)₂(TBP₈Cz) (18 – 29 μM) in CH₂Cl₂/py (99/1, v/v) or THF/py (99/1, v/v), was added one equiv of tetrabutylammonium borohydride (Bu₄NBH₄). The solution was stirred for 5 min and a color change of yellow-green to green was noted. The final green color was characteristic of the reduced Co^{II} species. An aliquot of this solution was transferred to a custom-made Schlenk cuvette and sealed. The solution was cooled to -65 °C in the cryostat, and 50 μL of an O₂-saturated CH₂Cl₂ solution was added. The reaction was monitored by UV-vis spectroscopy. The concomitant disappearance of the 612 and 764 nm peaks and the appearance of the 700 nm peak indicated the formation of the [Co^{III}(py)(O₂)(TBP₈Cz)]⁻ species.

b) ¹H NMR spectroscopy. To a solution of Co^{III}(py)₂(TBP₈Cz) (1.3 mM) in CD₂Cl₂/py-*d*₅ (20/1, v/v), was added one equiv of Bu₄NBH₄. The solution was stirred for 5 min and a color change of yellow-green to green was noted. The final green color was characteristic of the reduced Co^{II} species. An aliquot of this solution was transferred to an NMR tube and sealed. The solution was cooled to -65 °C in an acetone/liquid N₂ bath. NMR spectra of [Co^{II}(py)(TBP₈Cz)]⁻ were collected at 25 °C and -65 °C. The appearance of paramagnetic peaks (see Fig 4b) indicated formation of [Co^{II}(py)(TBP₈Cz)]⁻. An amount of O₂ was bubbled into the solution at -65 °C to generate [Co^{III}(py)(O₂)(TBP₈Cz)]⁻, and then sparged with Ar(g) to remove the excess O₂. The NMR spectrum of [Co^{III}(py)(O₂)(TBP₈Cz)]⁻ was collected at -65 °C.

c) EPR spectroscopy. To a solution of Co^{III}(py)₂(TBP₈Cz) (2.1 mM) in THF/py (20/1, v/v), was added one equiv of Bu₄NBH₄. The solution was stirred for 5 min and a color change of yellow-green to green was noted. The final green color was characteristic of the reduced Co^{II} species. An aliquot of this solution was transferred to an EPR tube and sealed. The solution was cooled to -65 °C in an acetone/liquid N₂ bath, and O₂ was bubbled into the solution to generate

[Co^{III}(py)(O₂)(TBP₈Cz)]⁻. The reaction mixture was then sparged with Ar_(g) to remove the excess O₂. The solution was rapidly frozen in liquid nitrogen prior to analysis by EPR spectroscopy. EPR parameters: T = 12 K, freq. = 9.43 GHz, power = 0.201 mW, mod. amp. = 10 G, mod. freq. = 100 kHz, receiver gain = 5.02 × 10³.

Reactivity with N–H substrates

a) Reaction of [Co^{III}(py)(O₂)(TBP₈Cz)]⁻ with phenylhydrazine. EPR Spectroscopy. To a solution of [Co^{III}(py)(O₂)(TBP₈Cz)]⁻ (2.1 mM) in CH₂Cl₂/py (20/1, v/v) at -65 °C, was added a solution of phenylhydrazine in CH₂Cl₂ (50 μL, 5.3 mmol, 50 equiv). The reaction mixture was allowed to react for 1 min and then frozen in liquid N₂ prior to analysis by EPR spectroscopy. EPR parameters: T = 12 K, freq. = 9.43 GHz, power = 0.201 mW, mod. amp. = 10 G, mod. freq. = 100 kHz, receiver gain = 5.02 × 10³.

b) Reaction of [Co^{III}(py)(O₂)(TBP₈Cz)]⁻ with DPH. ¹H NMR Spectroscopy. To two separate solutions of [Co^{III}(py)(O₂)(TBP₈Cz)]⁻ (1.3 mM, 500 μL) in CD₂Cl₂/py-*d*₅ (20/1, v/v) at -65 °C was added a solution of DPH in CD₂Cl₂: (a) 50 μL, 0.35 μmol, 1 equiv and (b) 100 μL, 0.70 μmol, 2 equiv. The reaction mixtures were allowed to react at low temperature for 1 h, after which time, an internal standard, 3,5-dimethylanisole (DMA) (3.33 μmol) was added to each solution and the ¹H NMR spectra were recorded at -65 °C. The peaks corresponding to the phenyl protons of the *p-tBu*-phenyl groups of Co^{III}(py)₂(TBP₈Cz) at 8.21 (d, 4H) and the phenyl protons of azobenzene at 7.99 ppm (d, 4H) were integrated versus the phenyl proton of DMA at 6.63 ppm (s, 1H). Two trials were performed. Average yields of two trials for Co^{III}(py)₂(TBP₈Cz) and azobenzene were 87% ± 12% and 93% ± 12% respectively, assuming a stoichiometry of 2:1 (Co^{III}(py)₂(TBP₈Cz) : azobenzene). A control reaction was prepared by mixing Bu₄NBH₄ (1.3 mM) with DPH (2 equiv) and excess O₂ in the absence of the cobalt complex. The excess O₂ was removed by sparging with Ar_(g) at -65 °C, and DMA (3.33 μmol) was added as internal standard. The NMR spectrum was recorded and showed only peaks of the starting material diphenylhydrazine.

c) Kinetics of the reaction of [Co^{III}(py)(O₂)(TBP₈Cz)]⁻ with DPH (¹H/²D) as monitored by UV-vis. An amount of DPH (~10 – 100 equiv) was added to a solution of [Co^{III}(py)(O₂)(TBP₈Cz)]⁻ (18 μM for DPH and 29 μM for DPH-*d*₂) in CH₂Cl₂/py (99/1, v/v). The reaction was monitored by UV-vis spectroscopy and showed the decay of [Co^{III}(py)(O₂)(TBP₈Cz)]⁻ (λ = 700 nm) and production of Co^{III}(py)₂(TBP₈Cz) (λ = 670 nm). The pseudo-first-order rate constants, *k*_{obs}, were obtained by nonlinear least-squares fitting of the growth of Co^{III}(py)₂(TBP₈Cz) (670 nm) and decay of [Co^{III}(py)(O₂)(TBP₈Cz)]⁻ (λ = 700 nm) plotted as absorbance (Abs) versus time (t). The data were fit to the equation Abs_t = Abs_f + (Abs₀ - Abs_f)exp(-*k*_{obs}*t*), where Abs₀ and Abs_f are initial and final absorbance, respectively. Pseudo-first order *k*_{obs} values were obtained and exhibited a linear correlation with substrate concentrations. Second-order rate constants (*k*₂) were obtained from the slope of the best-fit line from a plot of *k*_{obs} versus substrate concentration. Kinetics of reaction of [Co^{III}(py)(O₂)(TBP₈Cz)]⁻ with DPH at two other temperatures (-75 °C and -85 °C) were also monitored.

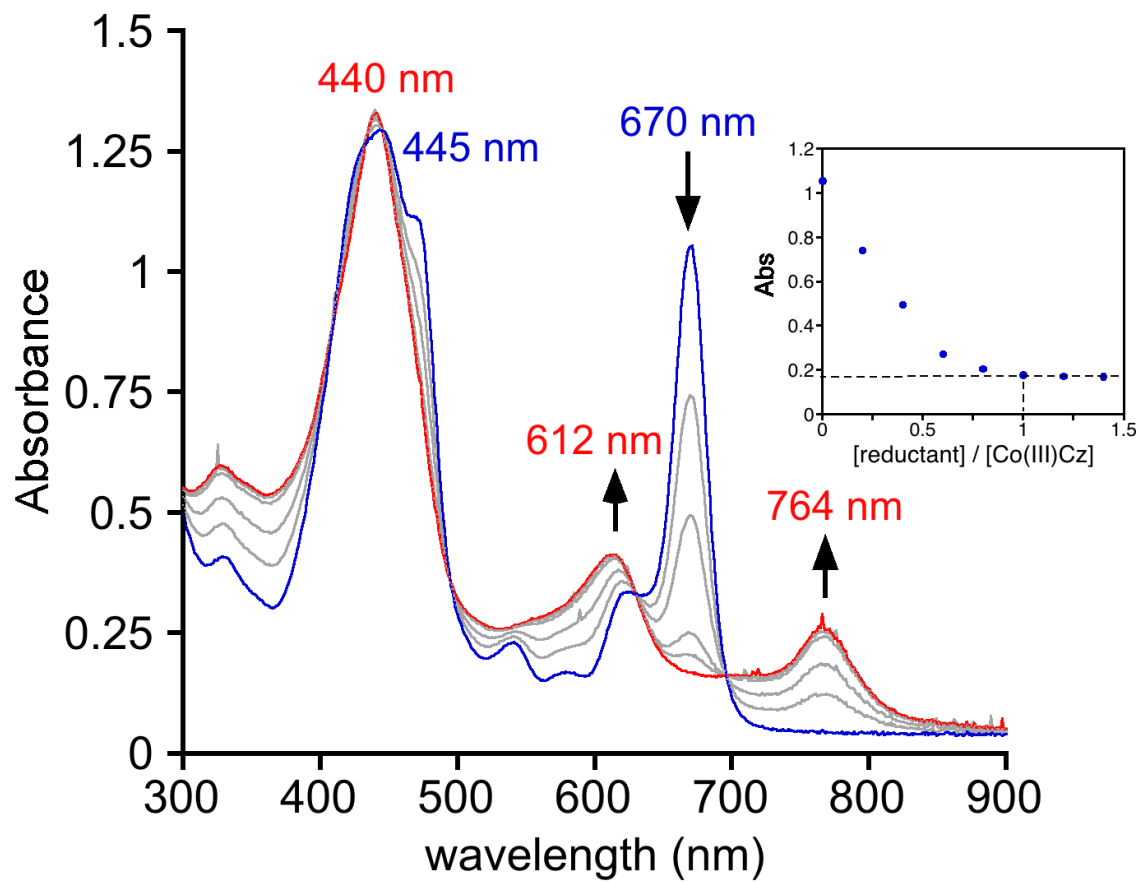


Figure S1. UV-vis spectral titration of $\text{Co}^{\text{III}}(\text{py})_2(\text{TBP}_8\text{Cz})$ (29 μM) with Bu_4NBH_4 (0 – 1 equiv) in $\text{CH}_2\text{Cl}_2/\text{py}$ (99/1, v/v) at 25 $^\circ\text{C}$.

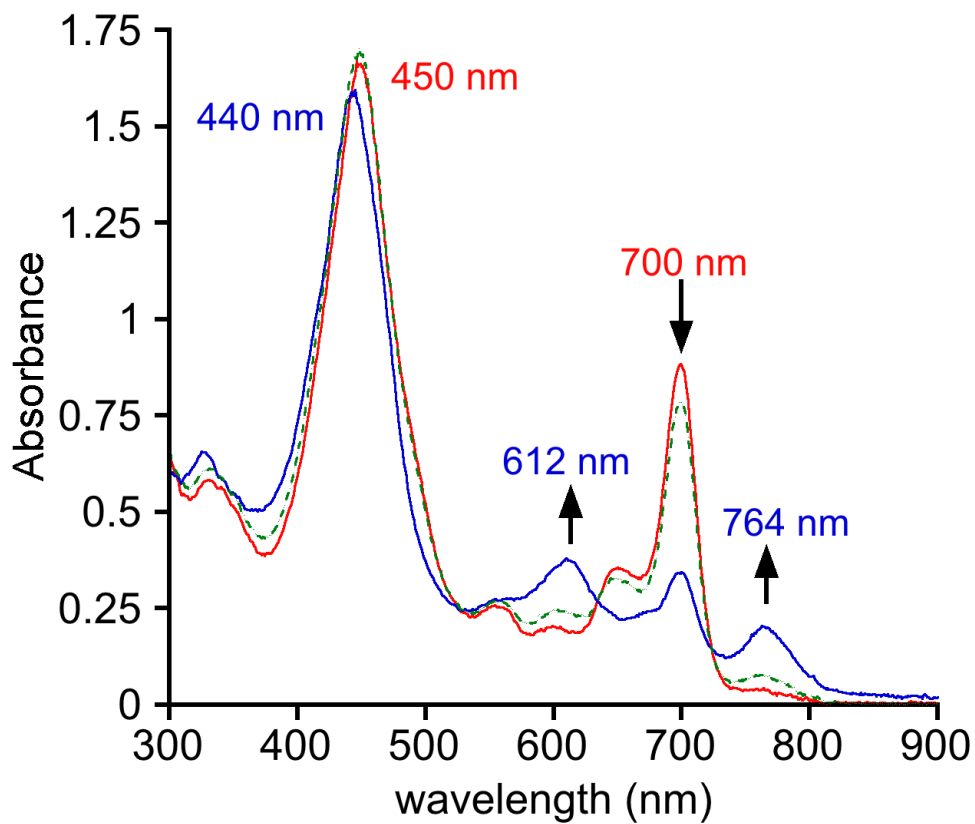


Figure S2. UV-vis spectra of $[\text{Co}^{\text{III}}(\text{py})(\text{O}_2)(\text{TBP}_8\text{Cz})]^-$ ($29 \mu\text{M}$) (red) after sparging with $\text{Ar}_{(\text{g})}$ (20 min) in $\text{CH}_2\text{Cl}_2/\text{py}$ (99/1, v/v) at $-65 \text{ }^\circ\text{C}$ (blue), and after regeneration by sparging with $\text{O}_{2(\text{g})}$ (green).

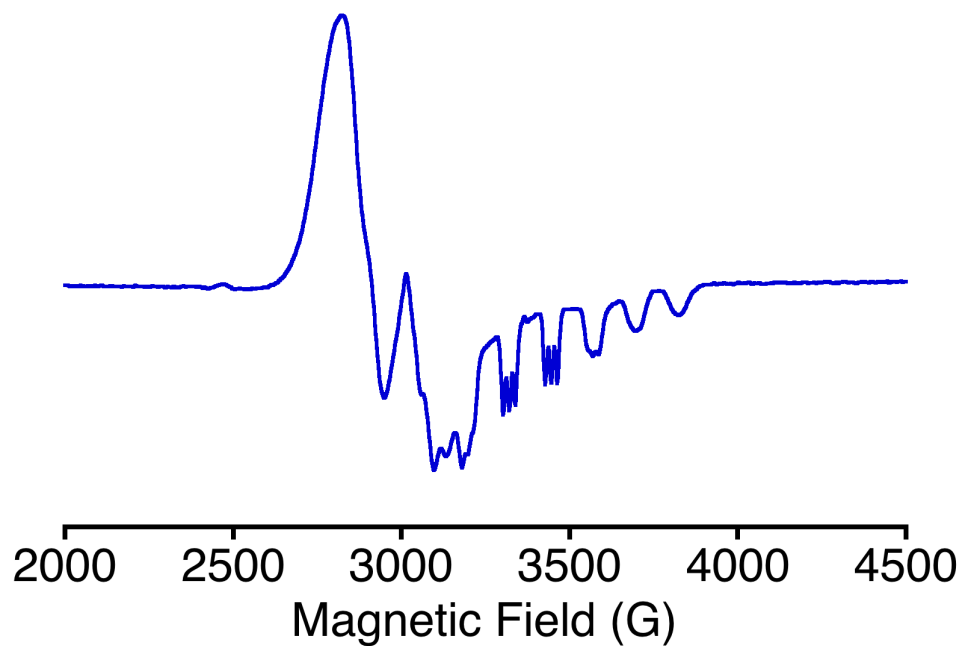


Figure S3. EPR spectrum of $[\text{Co}^{\text{II}}(\text{py})(\text{TBP}_8\text{Cz})]^-$ (2.1 mM) in THF/py (20/1, v/v). EPR parameters: $T = 12$ K, freq. = 9.43 GHz, power = 0.201 mW, mod. amp. = 10 G, mod. freq. = 100 kHz, receiver gain = 5.02×10^3 .

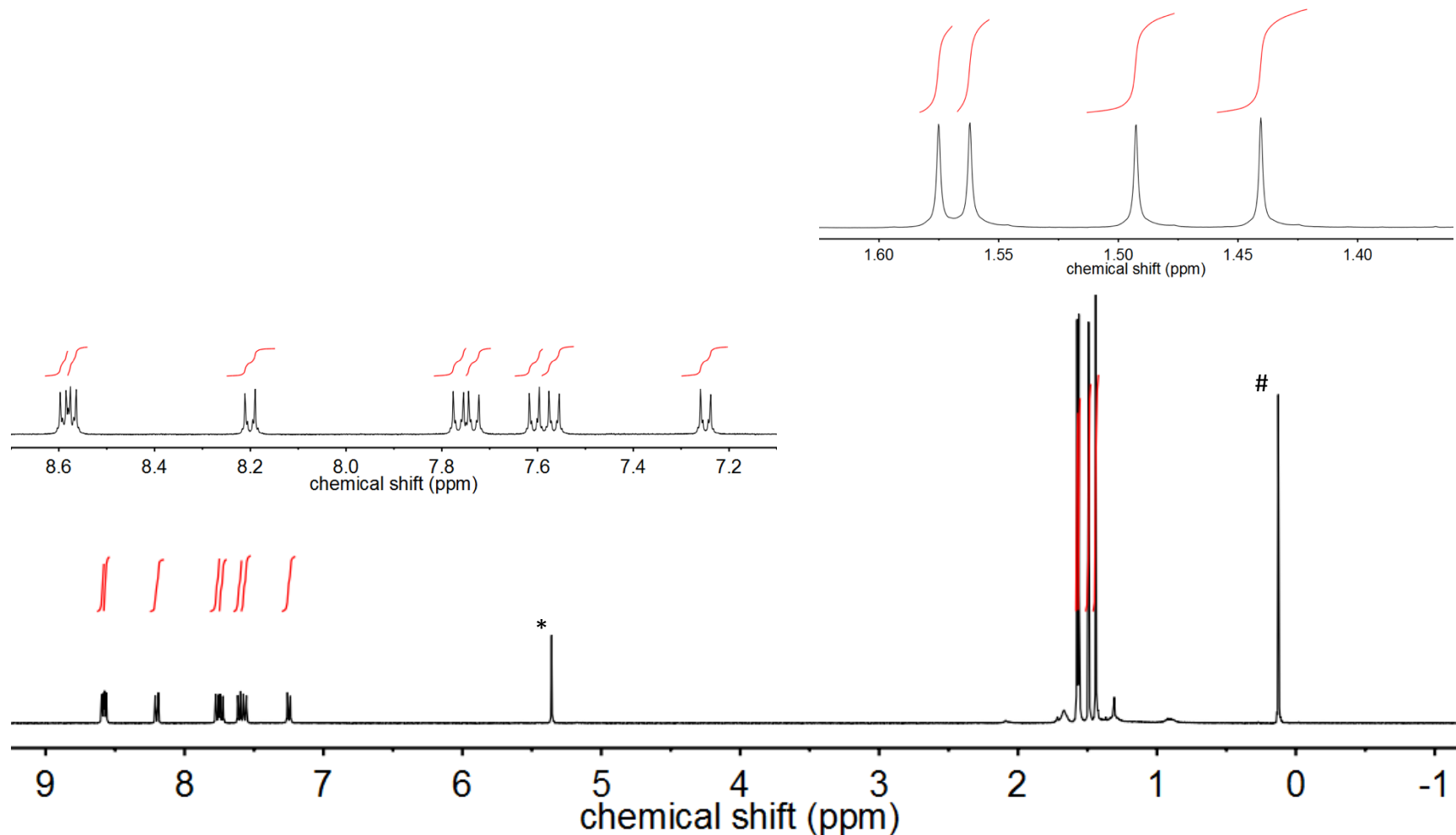


Figure S4a. ¹H NMR spectrum of Co^{III}(py)₂(TBP₈Cz) (1.3 mM) at 25 °C in CD₂Cl₂/py-d₅ (20/1, v/v). * = CH₂Cl₂, # = grease. ¹H NMR (400 MHz, CD₂Cl₂:py-d₅ (20:1, v/v)): δ (ppm) 8.59 (d, *J* = 8 Hz, 4H), 8.57 (d, *J* = 8 Hz, 4H), 8.21 (d, *J* = 8 Hz, 4H), 7.77 (d, *J* = 8 Hz, 4H), 7.73 (d, *J* = 8 Hz, 4H) 7.61 (d, *J* = 8 Hz, 4H), 7.57 (d, *J* = 8 Hz, 4H), 7.25 (d, *J* = 8 Hz, 4H), 1.58 (s, 18H), 1.56 (s, 18H), 1.49 (s, 18H), 1.44 (s, 18H).

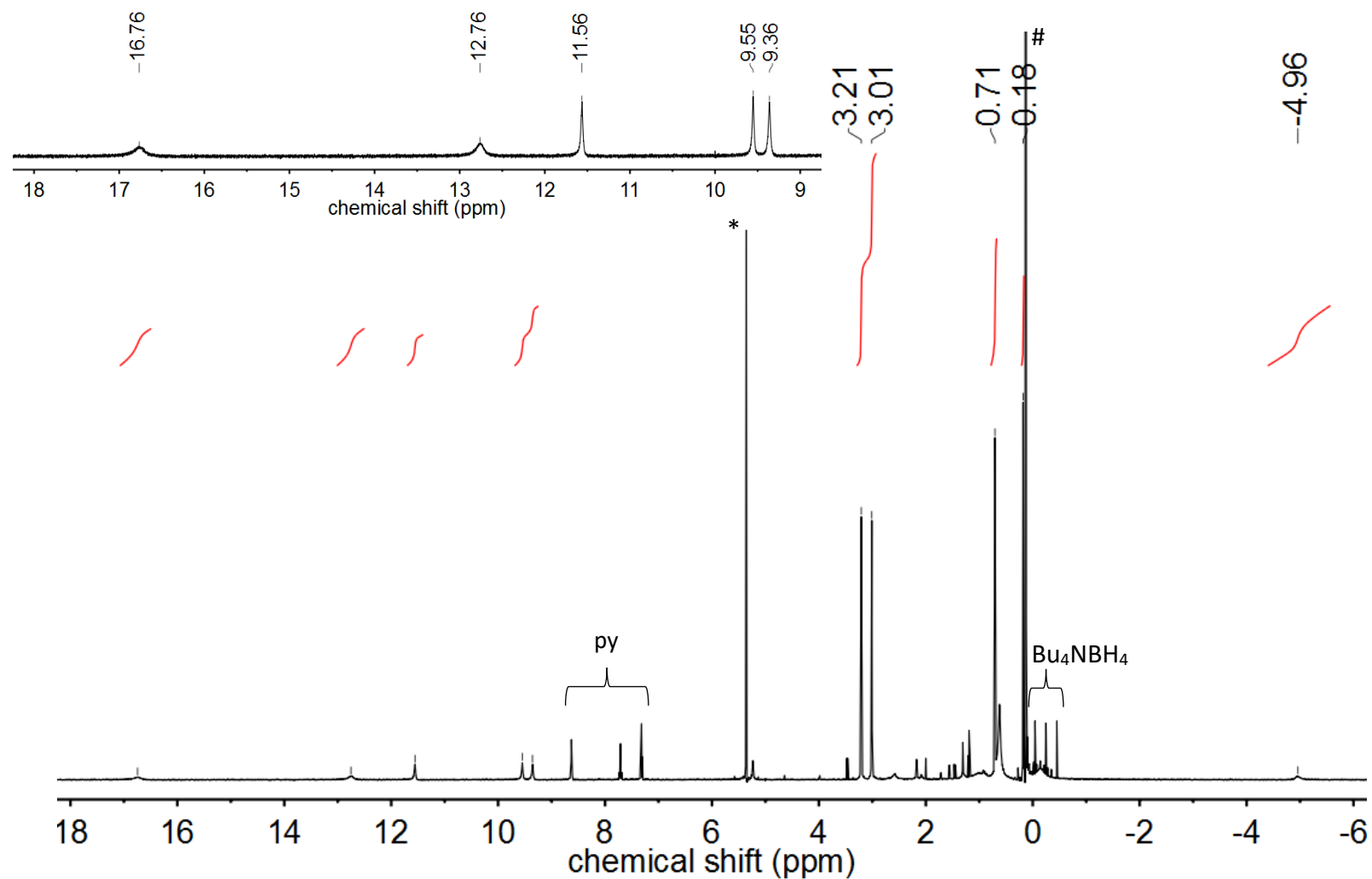


Figure S4b. ¹H NMR spectrum of [Co^{II}(py)(TBP₈Cz)]⁻ (1.3 mM) at 25 °C in CD₂Cl₂/py-*d*₅ (20/1, v/v). * = CH₂Cl₂, # = grease. ¹H NMR (400 MHz, CD₂Cl₂:py-*d*₅ (20:1, v:v)): δ (ppm) 16.76, 12.76, 11.56, 9.56, 9.36, 3.21, 3.01, 0.71, 0.18, -4.96.

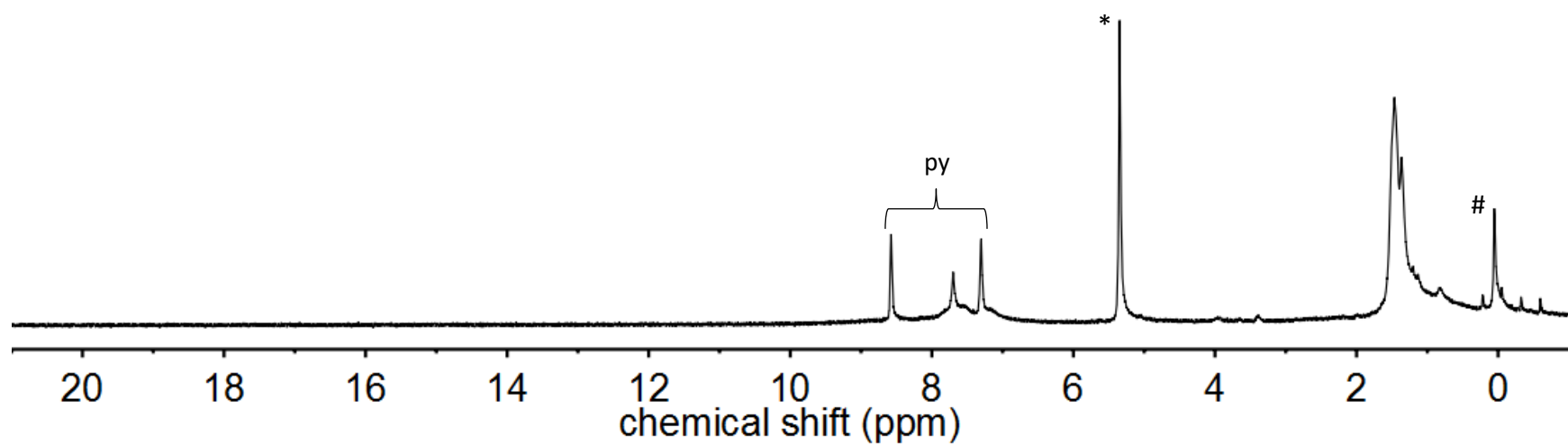


Figure S4c. ¹H NMR spectrum of [Co^{III}(py)(O₂)(TBP₈Cz)]⁻ (1.3 mM) at -65 °C in CD₂Cl₂/py-*d*₅ (20/1, v/v). * = CH₂Cl₂, # = grease.

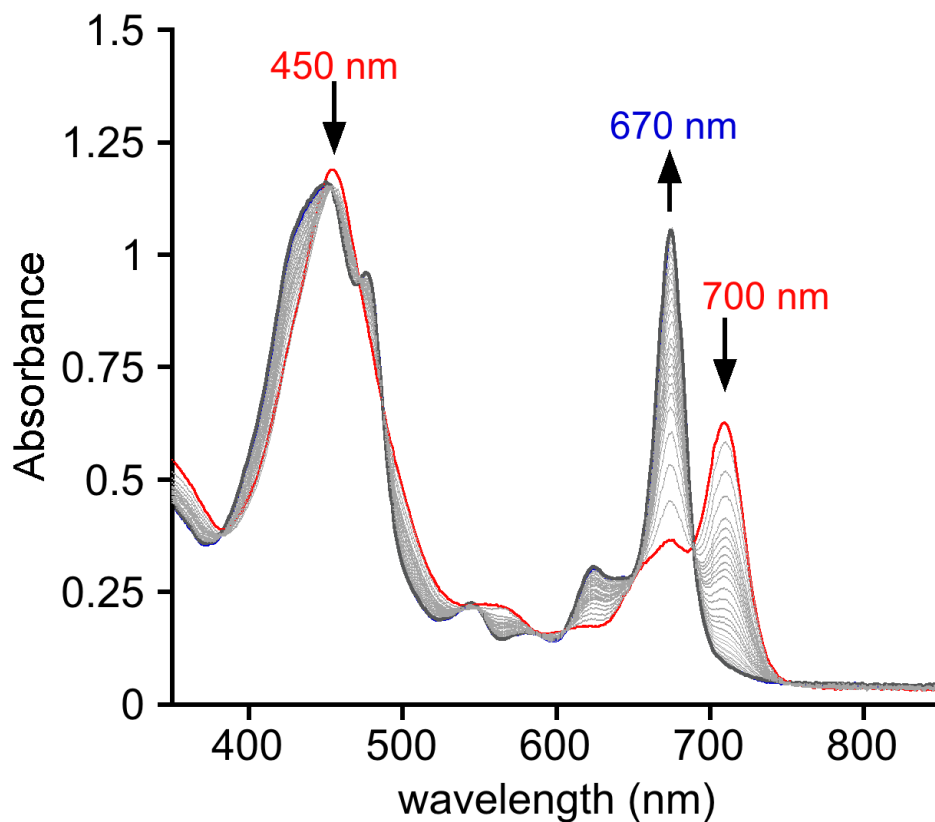


Figure S5. Time-resolved UV-vis spectral changes (0 – 70 min) observed for the reaction of $[\text{Co}^{\text{III}}(\text{py})(\text{O}_2)(\text{TBP}_8\text{Cz})]^-$ (18 μM) with TEMPOH (1573 equiv) to form $\text{Co}^{\text{III}}(\text{py})_2(\text{TBP}_8\text{Cz})$ in $\text{CH}_2\text{Cl}_2/\text{py}$ (99/1, v/v) at $-65\text{ }^\circ\text{C}$

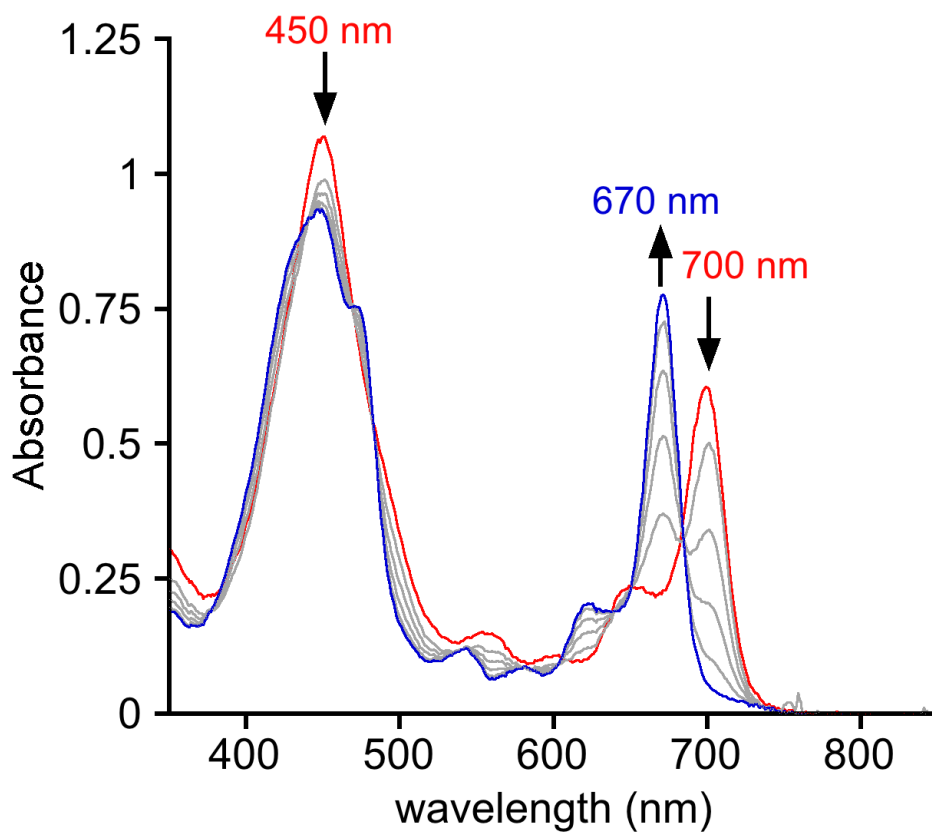


Figure S6. Time-resolved UV-vis spectral changes (0 – 5 min) observed for the reaction of $[\text{Co}^{\text{III}}(\text{py})(\text{O}_2)(\text{TBP}_8\text{Cz})]^-$ (18 μM) with PhNHNH_2 (222 equiv) to form $\text{Co}^{\text{III}}(\text{py})_2(\text{TBP}_8\text{Cz})$ in $\text{CH}_2\text{Cl}_2/\text{py}$ (99/1, v/v) at -65°C .

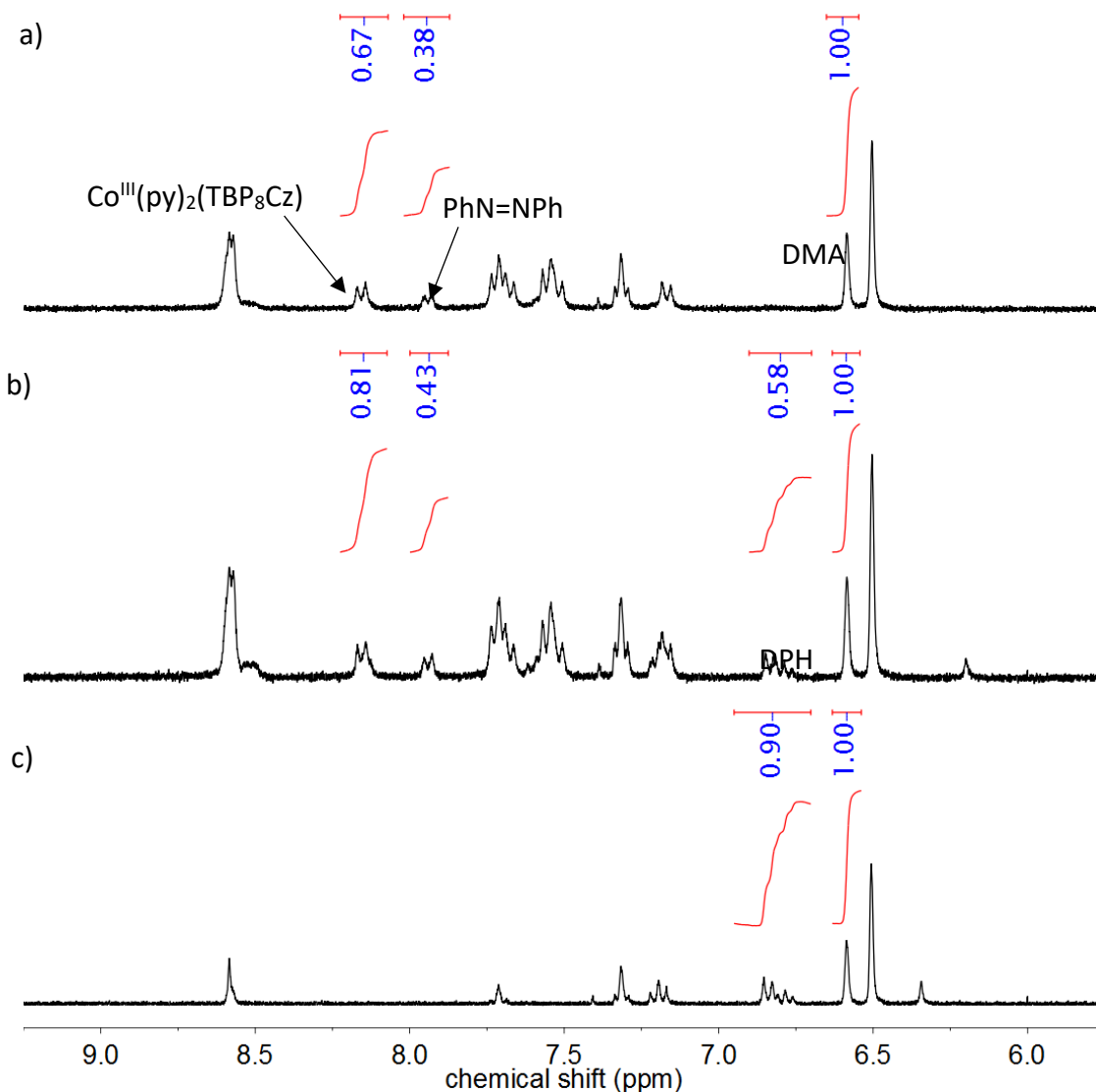


Figure S7. ^1H NMR spectra for the reaction of $[\text{Co}^{\text{III}}(\text{py})(\text{O}_2)(\text{TBP}_8\text{Cz})]^-$ (1.3 mM) with a) 1 equiv and b) 2 equiv of DPH in $\text{CD}_2\text{Cl}_2/\text{py}$ (20/1, v/v) to form $\text{Co}^{\text{III}}(\text{py})_2(\text{TBP}_8\text{Cz})$ and azobenzene ($\text{PhN}=\text{NPh}$). The peaks corresponding to the phenyl protons of the *p*-*t*Bu-phenyl groups of $\text{Co}^{\text{III}}(\text{py})_2(\text{TBP}_8\text{Cz})$ at 8.21 (d, 4H) and the phenyl protons of azobenzene at 7.99 ppm (d, 4H) were integrated versus the phenyl proton of DMA at 6.63 ppm (s, 1H). Two trials were performed. Average yields of two trials for $\text{Co}^{\text{III}}(\text{py})_2(\text{TBP}_8\text{Cz})$ and azobenzene were $87\% \pm 12\%$ and $93\% \pm 12\%$ respectively, assuming a stoichiometry of 2:1 ($\text{Co}^{\text{III}}(\text{py})_2(\text{TBP}_8\text{Cz})$: azobenzene), as computed using the formula below. For a separate control reaction (c), the NMR spectrum showed only peaks of the starting material diphenylhydrazine.

$$\% \text{ yield } \text{Co}^{\text{III}}(\text{py})_2(\text{TBP}_8\text{Cz}) = \frac{n_{\text{DMA}} \times \frac{I_{\text{Co}^{\text{III}}\text{Cz}} \times \frac{1}{4}}{I_{\text{DMA}}}}{n_{\text{Co}^{\text{III}}\text{Cz}_{\text{initial}}}} \times 100\%$$

$$\% \text{ yield azobenzene} = \frac{n_{\text{DMA}} \times \frac{I_{\text{azo}} \times \frac{1}{4} \times 2}{I_{\text{DMA}}}}{n_{\text{Co}^{\text{III}}\text{Cz}_{\text{initial}}}} \times 100\%$$

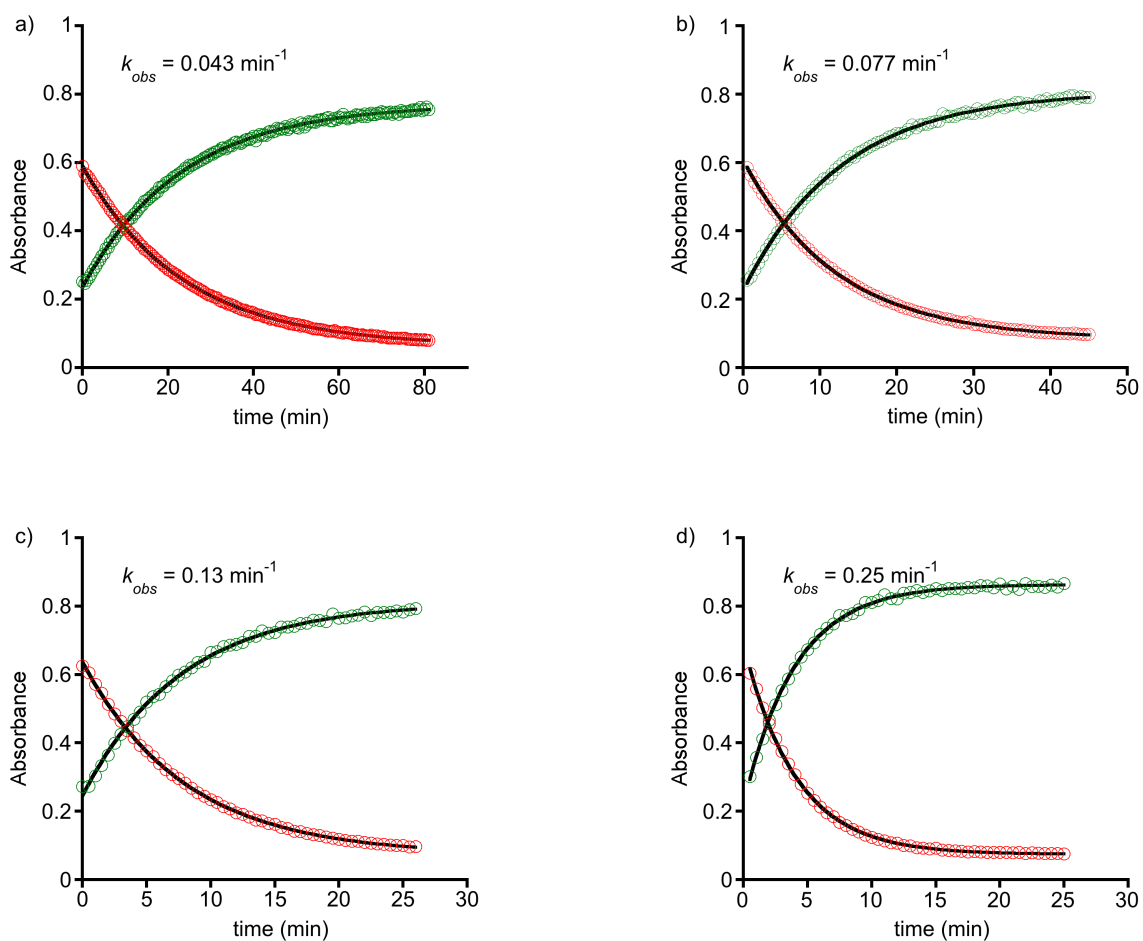


Figure S8. Plots of the change in absorbance vs time for the growth of $\text{Co}^{\text{III}}(\text{py})_2(\text{TBP}_8\text{Cz})$ (670 nm) (green) and decay of $[\text{Co}^{\text{III}}(\text{py})(\text{O}_2)(\text{TBP}_8\text{Cz})]^-$ (700 nm) (red) with the best fit lines for the reaction of $[\text{Co}^{\text{III}}(\text{py})(\text{O}_2)(\text{TBP}_8\text{Cz})]^-$ (18 μM) with DPH (a-d: 8, 18, 30, 61 equiv) in $\text{CH}_2\text{Cl}_2/\text{py}$ (99/1, v/v) at -65°C .

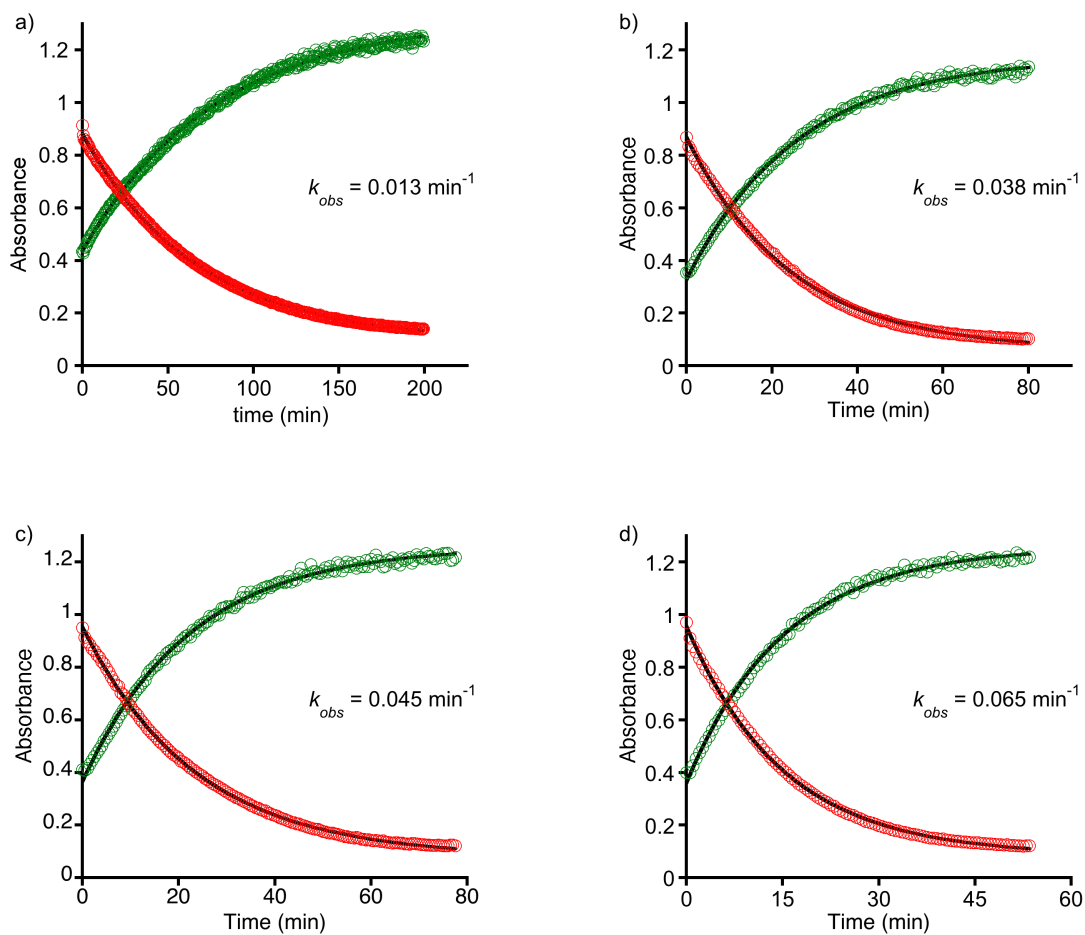


Figure S9. Plots of the change in absorbance vs time for the growth of $\text{Co}^{\text{III}}(\text{py})_2(\text{TBP}_8\text{Cz})$ (670 nm) (green) and decay of $[\text{Co}^{\text{III}}(\text{py})(\text{O}_2)(\text{TBP}_8\text{Cz})]^-$ (700 nm) (red) with the best fit lines for the reaction of $[\text{Co}^{\text{III}}(\text{py})(\text{O}_2)(\text{TBP}_8\text{Cz})]^-$ (29 μM) with DPH- d_2 (a-d: 19, 48, 69, 93 equiv) in $\text{CH}_2\text{Cl}_2/\text{py}$ (99/1, v/v) at -65°C .

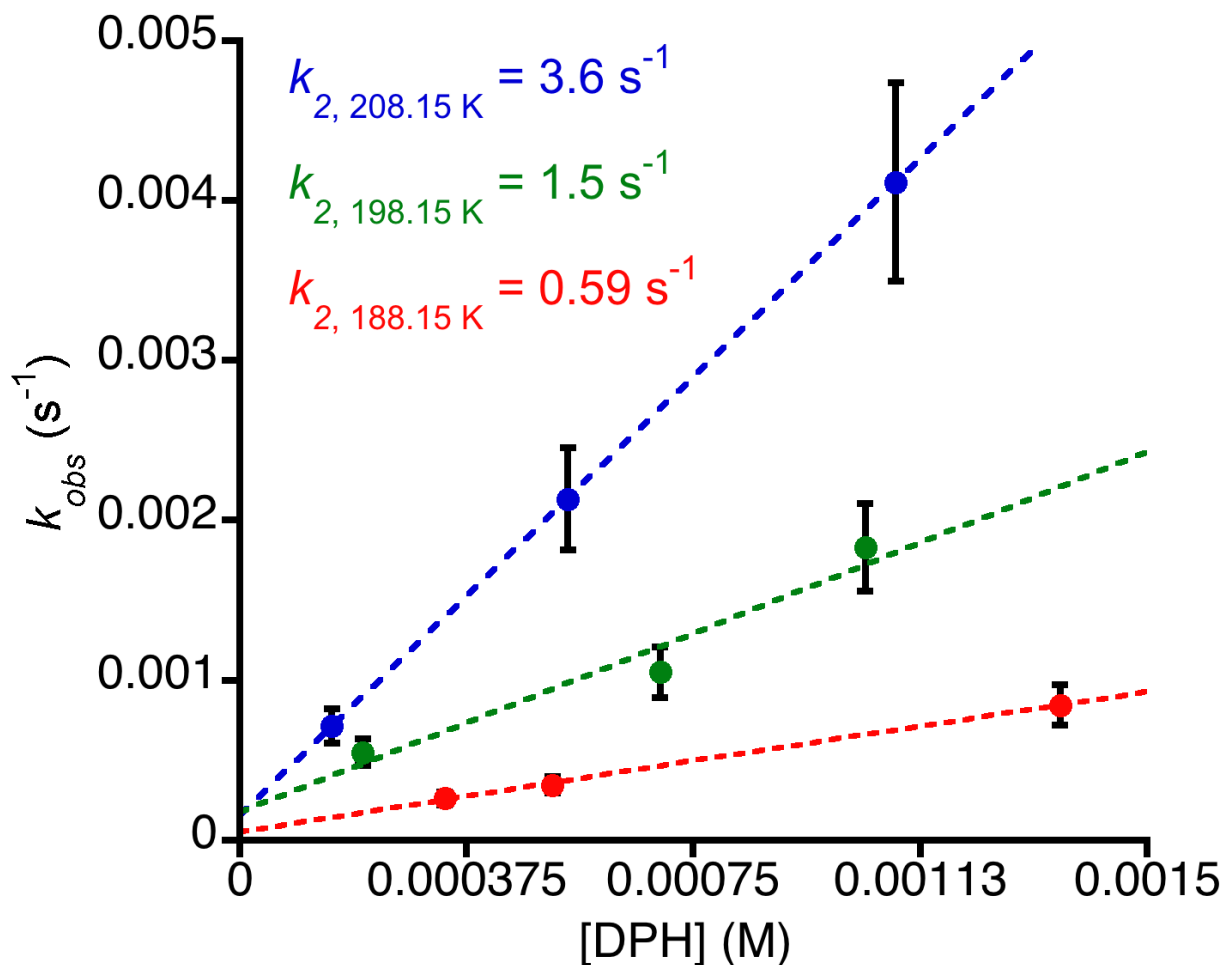


Figure S10. Plots of pseudo-first-order rate constants (k_{obs}) versus [DPH] with best fit lines at -65 °C (blue), -75 °C (green), -85 °C (red).

1. E. E. Joslin, J. P. Zaragoza, R. A. Baglia, M. A. Siegler and D. P. Goldberg, *Inorg. Chem.*, 2016, **55**, 8646-8660.
2. B. Ramdhanie, L. N. Zakharov, A. L. Rheingold and D. P. Goldberg, *Inorg. Chem.*, 2002, **41**, 4105-4107.
3. S. Marque, H. Fischer, E. Baier and A. Studer, *J. Org. Chem.*, 2001, **66**, 1146-1156.